



**Synthesis, Structures, and Reactivity Studies of
Cyclometalated N-Heterocyclic Carbene Complexes of
Ruthenium**

| | |
|-------------------------------|----------------------------------------------------------------------------------------------------------------------------------------------------------------------------------------------------------------------------------------------------|
| Journal: | <i>Dalton Transactions</i> |
| Manuscript ID | DT-ART-05-2018-001925.R1 |
| Article Type: | Paper |
| Date Submitted by the Author: | 06-Jul-2018 |
| Complete List of Authors: | Liu, Hsueh-Ju; National Chiao Tung University, Department of Applied Chemistry Ziegler, Micah; Massachusetts Institute of Technology, Institute for Data, Systems, and Society Tilley, T. Don; University of California, Berkeley, Chemistry |
| | |



Journal Name

Synthesis, Structures, and Reactivity Studies of Cyclometalated N-Heterocyclic Carbene Complexes of Ruthenium†

Received 00th January 20xx,
Accepted 00th January 20xx

Hsueh-Ju Liu,^{a,b} Micah S. Ziegler^{a,c} and T. Don Tilley^{*a}

DOI: 10.1039/x0xx00000x

www.rsc.org/

An unusual cyclometalation reaction results from a C–C bond activation in Cp*(IPr)RuCl to give Cp*(IPr')Ru(L) featuring a NHC-C(sp²) chelating ligand (**5-L**; L = propene, N₂; IPr = 1,3-bis(2,6-diisopropylphenyl)imidazol-2-ylidene; IPr' = 1-(6-isopropylphenyl)-3-(2,6-diisopropylphenyl)imidazol-2-ylidene). DFT calculations were carried out to elucidate the C–C bond activation pathway. Reactions of cyclometalated ruthenium complexes bearing NHC-C(sp²) and NHC-C(sp³) ligands (**5-L** and Cp*(IXy-H)Ru(N₂), **1a**, respectively) where IXy = 1,3-bis(2,6-dimethylphenyl)imidazol-2-ylidene; IXy-H is the deprotonated form of IXy) are reported. Deprotonation of **1a** by an equimolar mixture of benzyl potassium and 18-crown-6 afforded a doubly-cyclometalated complex [Cp*(IXy-2H)Ru][K(18-crown-6)] (**7**). A lower CO stretching frequency in Cp*(IXy-H)Ru(CO) (**8**) vs. Cp*(IPr')Ru(CO) (**9**) suggests that the NHC-C(sp³) ligand is more electron donating. Complexes **5-L** react with H₂ to give the dihydride Cp*(IPr')RuH₂ (**11**). In comparison, after an initial oxidative addition of H₂, complex **1a** with its more reactive Ru–C(sp³) bond undergoes C–H reductive elimination, and a second oxidative addition of H₂ afforded the trihydride Cp*(IXy)RuH₃ (**10**). Reaction of **1a** with B(C₆F₅)₃ resulted in a zwitterionic complex Cp*Ru(IXy'') (**12**; IXy'' = 1-[2-((C₆F₅)₂CH₂)C₆H₃-6-methyl]-3-(2,6-dimethylphenyl)imidazol-2-ylidene-1-yl) by the formation of a new C–B bond. In contrast, B(C₆F₅)₃ abstracted a hydride from **5-L** and promoted a very unusual C–C bond formation involving insertion of an allyl ligand into a Ru–C bond to form [Cp*Ru(IPr'')][H(B(C₆F₅)₃)] (IPr'' = 1-[2-(CH₂=CHCH₂)C₆H₃-6-isopropyl]-3-(2,6-diisopropyl)imidazol-2-ylidene-1-yl) (**13**).

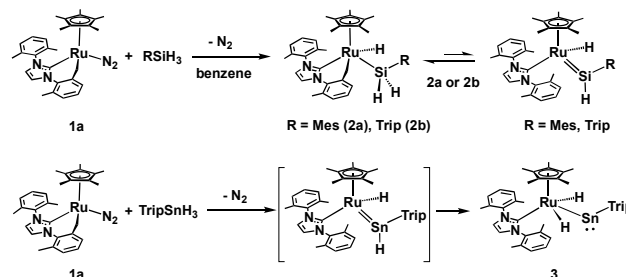
Introduction

Cyclometalation, the intramolecular metalation of a ligand to form a chelate ring, often introduces a metal-carbon σ bond and provides access to a wide range of metallacyclic transition metal complexes.^{1, 2} Some cyclometalated complexes have attracted attention in applications as catalyst precursors or catalytic intermediates.^{3–5} In particular, cyclometalated ruthenium complexes have proven to be versatile synthetic precursors^{6, 7} and effective catalysts for hydrogen transfers, hydrogenations, and olefin metathesis.^{8, 9} In addition, since cyclometalated complexes can possess reactive metal-ligand interactions as part of a strained ring, they have the potential to cleave a range of element–H bonds in conversions that can be thermodynamically driven by the formation of strong C–H or C–E (E = Si, B) bonds.^{5, 10, 11}

Previously, we described the synthesis and reactivity of the NHC-cyclometalated complex Cp*(IXy-H)Ru (**1**) and its dinitrogen adduct Cp*(IXy-H)Ru(N₂) (**1a**) [IXy = 1,3-bis(2,6-dimethylphenyl)imidazol-2-ylidene; IXy-H is deprotonated IXy; Cp* = C₅Me₅],¹² which were

obtained *via* dehydrochlorination of Cp*(IXy)RuCl with benzyl potassium (1 equiv). In benzene-*d*₆ at 24 °C, complex **1** exhibits chemically equivalent xylyl substituents on the NMR time-scale, consistent with a reversible, intramolecular C–H activation process that transfers hydrogen between the xylyl methyl groups. Moreover, upon N₂ dissociation, **1a** activates Si–H and Sn–H bonds to produce Cp*(IXy-H)(H)RuSiH₂R [R = Mes (**2a**), or Trip (**2b**)], (Mes = 2,4,6-trimethylphenyl; Trip = 2,4,6-triisopropylphenyl)^{12, 13} and the ruthenostannylene complex Cp*(IXy)(H)₂Ru–SnTrip (**3**),¹⁴ respectively (Scheme 1). Both **2a** and **2b** rapidly equilibrate with their corresponding silylene isomers *via* a sequence of C–H bond elimination and α-H migration steps.^{12, 13}

Scheme 1. Activation of organosilanes and an organostannane by complex **1a**



The synthesis of **1a** exemplifies a common synthetic route to cyclometalated complexes involving C–H activation of a ligand substituent. Metal-hydride and -alkyl complexes are well known to undergo the activation of ligand C–H bonds in cyclometalations that eliminate H₂ or a hydrocarbon, respectively, *via* σ-bond metathesis

^a Department of Chemistry, University of California, Berkeley, Berkeley, California 94720-1460, USA.

^b Current address: Department of Applied Chemistry, National Chiao Tung University, No 1001, Daxue Rd, Hsinchu, Taiwan 30010.

^c Current address: Institute for Data, Systems, and Society, Massachusetts Institute of Technology, Cambridge, Massachusetts 02139, USA

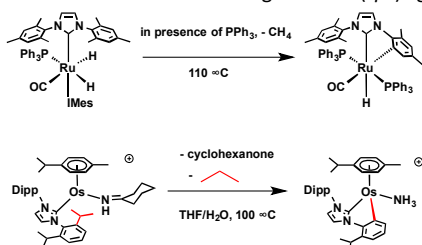
† This manuscript is dedicated to Professor Richard A. Andersen on the occasion of his 75th birthday.

Electronic Supplementary Information (ESI) available: [details of any supplementary information available should be included here]. See DOI: 10.1039/x0xx00000x

or an oxidative addition/reductive elimination sequence. Notably, Whittlesey and coworkers have shown that metal complexes featuring hydride ligands or a low-valent metal center are particularly prone to cyclometalation.^{8, 15-17}

Cyclometalations involving activation of C–C bonds are much more rare, likely due to the relative kinetic inertness of C–C (vs. C–H) bonds. In one such case, Whittlesey and co-workers demonstrated the direct C–C bond activation of the IMes (IMes = 1,3-bis(2,4,6-trimethylphenyl)imidazol-2-ylidene) ligand in $\text{RuH}_2(\text{CO})(\text{IMes})_2(\text{PPh}_3)$ at 110 °C in the presence of free PPh_3 , to yield a ruthenium complex featuring a chelating $\text{NHC-C}(sp^2)$ ligand.¹⁵ More recently, Bolaño *et al.* reported that thermal decomposition of the osmium complex $[(\eta^6\text{-}p\text{-cymene})\text{Os}(\text{NHCy})(\text{IPr})]\text{BF}_4$ (IPr = 1,3-bis(2,6-diisopropylphenyl)imidazol-2-ylidene) at 100 °C in moist THF affords a new osmium complex along with propane in a process involving C–C bond activation (Scheme 2).¹⁸

Scheme 2. C–C bond activation resulting in $\text{NHC-C}(sp^2)$ ligands^{15, 18}



Herein we report an unusual activation of an unstrained C–C bond of the IPr ligand in $\text{Cp}^*(\text{IPr})\text{RuCl}$, resulting in a cyclometalated mixture of products (**5-L**), and the mechanistic investigation of this C–C bond activation event by DFT calculations. In addition, reactions of the cyclometalated complexes **1a** and **5-L** with substrates including H_2 , mesitylsilane (MesSiH_3) and $\text{B}(\text{C}_6\text{F}_5)_3$ were explored, revealing distinct reactivities for in Cp^*Ru complexes featuring $\text{NHC-C}(sp^3)$ (**1a**) vs. $\text{NHC-C}(sp^2)$ (**5-L**; L = N_2 , propene) ligands.

Results and discussion

Cyclometalations in $\text{Cp}^*(\text{IPr})\text{Ru}$ complexes. With the initial goal of synthesizing $\text{Cp}^*(\text{IPr})\text{Ru}$ -alkyl complexes as precursors to unsaturated metal-silicon species,¹⁹ salt metathesis of $\text{Cp}^*(\text{IPr})\text{RuCl}$ with potential alkylating reagents was investigated. Unlike the aforementioned reaction of $\text{Cp}^*(\text{IXy})\text{RuCl}$,¹² treatments of $\text{Cp}^*(\text{IPr})\text{RuCl}$ with one equivalent of KCH_2Ph , MeLi , or $\text{Mg}(\text{CH}_2\text{Ph})_2$ in benzene at 24 °C did not afford clean products. However, the reaction of $\text{Cp}^*(\text{IPr})\text{RuCl}$ with one equivalent of $\text{LiCH}_2\text{SiMe}_3$ in benzene- d_6 at 24 °C produced within five minutes a navy blue intermediate, along with one equiv of SiMe_4 as determined by ^1H NMR spectroscopy. A representative spectrum of this blue intermediate (Figure 1) exhibits three resonances assignable to i Pr methine protons and six doublet resonances for methyl groups, suggesting the presence of three inequivalent isopropyl groups. Notably, the absence of one methine proton and the presence of a

simple singlet assignable by integration to a methyl group (2.02 ppm) suggest that C–H activation at the methine carbon forms a six-membered metallacycle (**4a**, Figure 1); a related methyl group appears to be obscured by other peaks grouped into the region of 1.0 - 1.8 ppm (*vide infra*). After 24 hours, the solution color faded to pale yellow and the ^1H NMR spectrum revealed that **4a** had transformed into a mixture of multiple Cp^*Ru -containing products, with the release of a small amount of propene.

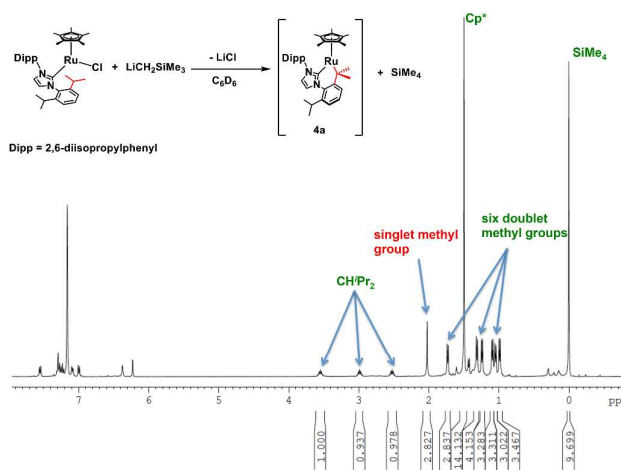
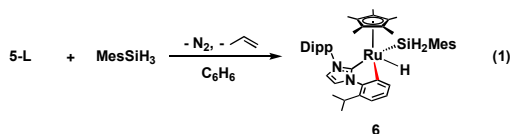


Figure 1. Formation of **4a** by reaction of $\text{Cp}^*(\text{IPr})\text{RuCl}$ with $\text{LiCH}_2\text{SiMe}_3$ in benzene- d_6 at 24 °C after 5 mins, as evidenced by ^1H NMR spectroscopy.

The resulting product mixture was isolated as a yellow powder upon evaporation of a pentane extract. A ^1H NMR spectrum of this product mixture (benzene- d_6 , 24 °C) exhibits three Cp^* resonances in a 1:2.6:3.5 ratio, consistent with formation of at least three Cp^*Ru -containing products, collectively denoted **5-L**. Due to their similar solubilities, separation of this mixture into its components was not possible. The product mixture **5-L** was analyzed by mass spectrometry (EI, electron ionization) which showed a parent ion peak with a m/z value of 624, corresponding to that expected for dehydrochlorination of $[\text{Cp}^*(\text{IPr})\text{RuCl}]$. In addition, the infrared spectrum of this mixture reveals a $\nu(\text{N}_2)$ stretching frequency at 2093 cm^{-1} , suggesting that at least one component of **5-L** features dinitrogen bound to Ru. While numerous attempts to grow X-ray quality crystals from the **5-L** mixture were unsuccessful, reactivity studies (*vide infra*) designed to further elucidate the nature of these complexes suggest that they are very similar and likely complexes of N_2 and propene.

Evidence for the composition of **5-L** was initially obtained by examination of the reaction with mesitylsilane. Treatment of the product mixture **5-L** with excess MesSiH_3 in benzene- d_6 at 24 °C resulted in clean formation of a single ruthenium silyl hydride complex (**6**) as evidenced by ^1H NMR spectroscopy. The ^1H NMR spectrum exhibits one resonance at -9.50 ppm that integrates as one hydrogen and is assigned as a Ru-bound hydride, and resonances at 4.79 and 4.58 ppm (one H each) are assigned as two

Si-bound hydrogens. Additionally, three resonances in the alkene region (5–6 ppm) indicate formation of approximately 0.5 equivalents of propene (eq 1).²⁰



Crystals of **6** were obtained by cooling a pentane solution to $-35\text{ }^{\circ}\text{C}$, and X-ray crystallography (Figure 2) confirmed the complex to be a silyl hydride, with Ru–H and Ru–Si bond lengths of 1.56(3) and Ru–Si 2.3958(8) Å, respectively. A rather long silyl-hydride interligand distance of 2.12(2) Å and an unobserved J_{SiH} coupling constant (< 7 Hz) in the ^1H NMR spectrum are consistent with **6** being a classical, ruthenium(IV) silyl hydride complex.^{21–23} Notably, the modified IPr' ligand (1-(6-isopropylphenyl)-3-(2,6-diisopropylphenyl)imidazol-2-ylidene) was found to bind to ruthenium through both the central

carbene and a cyclometalated-aryl carbon, forming a five-membered chelate ring with Ru–C1(carbene) and Ru–C3(aryl) bond lengths of 2.020(3) and 2.093(3) Å, respectively.

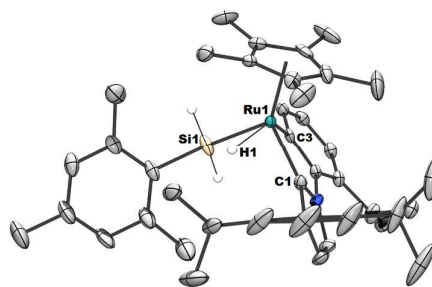


Figure 2. Molecular structure of **6** displaying thermal ellipsoids at the 50% probability level. Selected H atoms have been omitted for clarity.

Scheme 3. Mechanistic study of the C–C bond activation by DFT calculations.

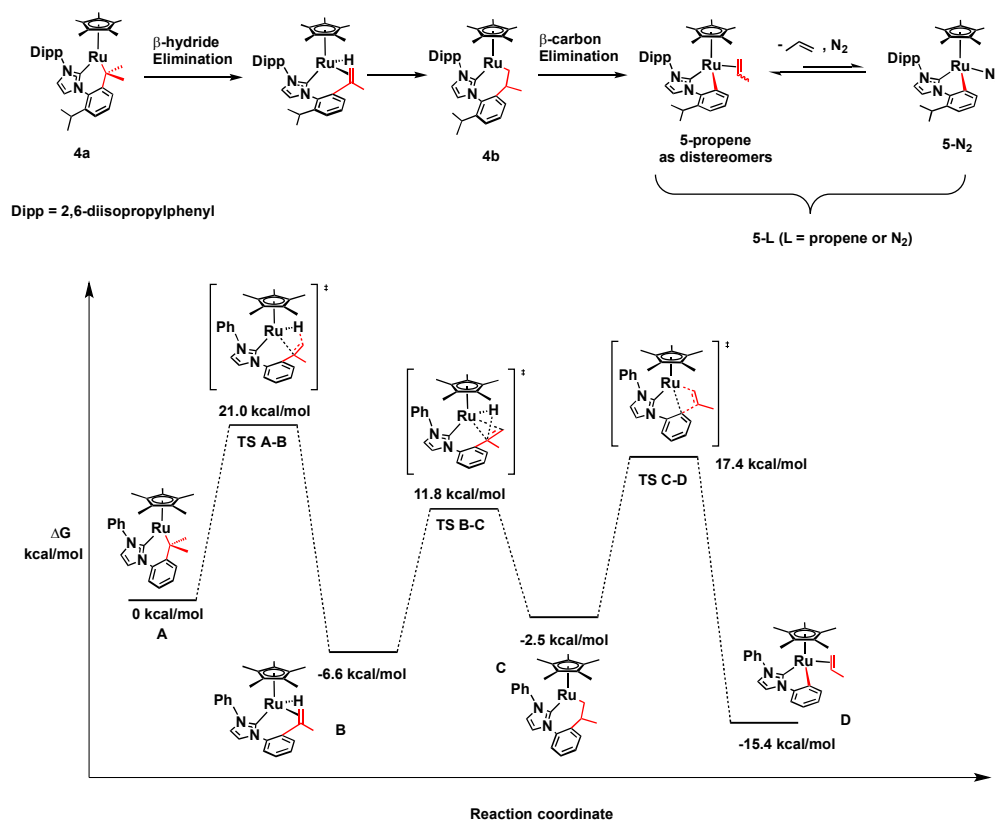


Figure 3. Gibbs free energy profile for the formation of **D**.

The formation of the IPr' ligand, as evidenced by structural analysis of **6**, suggests that the conversion of **4a** to **5-L** involves C–C bond activation, and that **5-L** is likely composed of cyclometalated

products resulting from this activation. These results can be explained by a process whereby **4a** undergoes β -hydride elimination and migratory insertion to yield **4b**, an isomer of **4a**

with a seven-membered metallacycle, as illustrating in Scheme 3. Then, *via* β -carbon elimination, **4b** yields the diastereomeric complexes **5-propene** (with different orientations of the propene methyl group), which in turn are in equilibrium with **5-N₂**, where the bound propene is replaced by dinitrogen. This equilibrium is evidenced by the observation of propene in the ¹H NMR spectrum of the benzene-*d*₆ solution of **5-L**.

DFT Analysis of Reaction Pathway Leading to the Formation of Complexes 5-L. To better understand this decomposition mechanism, DFT calculations at the B3LYP level of theory were employed to study the C–C bond cleavage process (see Figure 3 and Computational Details in Experimental section). First, the transformation of **A** (a slightly abbreviated analog of **4a**) to **D** (analogous to **5-propene**) is exoergic by 15.4 kcal/mol and consistent with the spontaneous decomposition to **5-L**. The formation of **D** starts with a thermodynamically favorable β -hydride elimination from 16-electron **A** to 18-electron olefin complex **B** *via* a located transition state **TS A-B** with an activation barrier of 21.0 kcal/mol. Complex **B** undergoes migratory insertion to form the isomeric, cyclometalated complex **C**. Finally, a concerted β -carbon elimination process leading to Ru–C(*sp*²) bond formation and C(*sp*²)–C(*sp*³) bond cleavage was found to proceed through transition state **TS C-D** to give the final product **D**. These calculations suggest that these complexes can undergo C–C bond activation with relatively low energetic barriers.

Doubly-metallated complex 7. While optimizing the synthesis of complex **1a** from Cp*(IXy)RuCl, excess KCH₂Ph was employed in an attempt to drive the reaction to completion. Surprisingly, the yield of **1a** decreased dramatically to 4% upon treatment with two equivalents of KCH₂Ph, suggesting that a second equivalent of KCH₂Ph reacts with newly formed **1a**. Indeed, addition of a clear, orange toluene solution of KCH₂Ph and 18-crown-6 (one equivalent for each) to a toluene solution of **1a** at 24 °C resulted in clean formation of [Cp*(IXy-2H)Ru][K(18-crown-6)] (**7**) in 97% yield (eq 2). Crystals suitable for X-ray crystallography were grown by diffusion of pentane into a saturated THF solution of **7**, and structure determination revealed a doubly-cyclometalated anionic complex with Ru–C bonds of 2.150(3) and 2.164(3) Å, and a C–Ru–C bond angle of 87.2(1)° (Figure 4), along with the [(THF)₂K(18-crown-6)]⁺ cation. The structure of **7** is reminiscent of the previously reported polymeric complex [Cp*Ru(IXy-2H)]Li, synthesized from the reaction of **1a** with LiCH₂SiMe₃, in which a doubly-cyclometalated Ru complex binds *via* the Ru-bound carbon atoms to a Li⁺ ion which in turn also coordinates the Cp* ring from another complex.²⁴ For comparison, reactions of the free NHCs IPr,²⁵ I^tBu,²⁵ and IXy²⁴ with strong bases led only to deprotonation of the imidazoylidene rings. Moreover, cyclic voltammetry of **7** in THF revealed a reversible one-electron redox event at E_{1/2} = –0.90 V (vs. [Cp₂Fe]^{0/1+}) assigned to the Ru(II)/Ru(III) couple, suggesting the accessibility of a 17-electron, neutral Cp*Ru(IXy-2H) complex. Complex **7** represents an intriguing starting material, which could induce two bond activations in a substrate, *via* two ring-opening processes involving

hydrogen transfer to both methylene groups of the ligand. This possibility is currently being investigated.

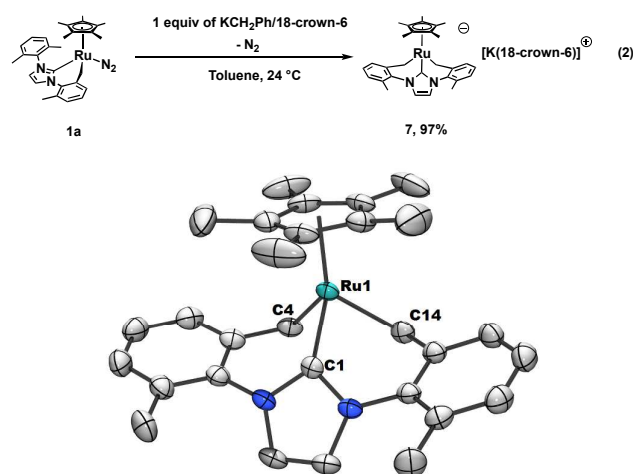
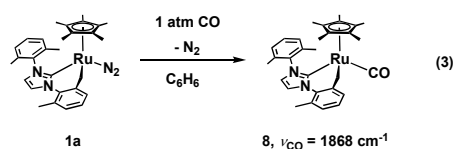
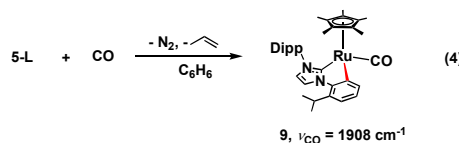


Figure 4. Anion of **7** displaying thermal ellipsoids at the 50% probability level. The cation, [K(18-crown-6)(THF)₂], three lattice THF molecules and H atoms have been omitted for clarity.

Carbonyl complexes with cyclometalated NHC ligands. To investigate the electronic properties of cyclometalated NHC ligands in the complexes described above, analogues containing carbonyl ligands were synthesized and characterized by IR spectroscopy. Under one atmosphere of CO at 24 °C, a brown benzene solution of **1a** became yellow within ten minutes and the corresponding complex Cp*(IXy-H)Ru(CO) (**8**; eq 3) was obtained as an analytically pure solid in 71% yield after removal of the volatile components *in vacuo* and recrystallization from pentane.



Similarly, exposure of **5-L** to one atmosphere of CO led to the formation of Cp*(IPr')Ru(CO) (**9**; eq 4). By ¹H NMR spectroscopy, this reaction liberated ~0.5 equiv of propene and resulted in quantitative conversion of all components of **5-L** to **9**, as evidenced by consumption of all three Cp* resonances.

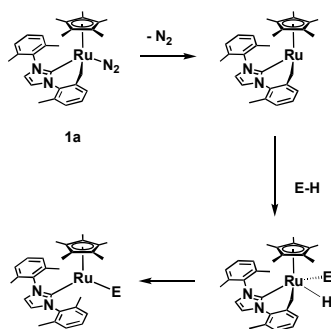


The carbonyl stretching frequency of **8** (1868 cm⁻¹) is significantly lower than that of **9** (1908 cm⁻¹). A similar effect is found in comparing the ν (N₂) stretching frequency of **1a** (2069 cm⁻¹) to that of **5-N₂** (2093 cm⁻¹). Both trends are consistent with stronger

electron donation to the Ru center, and subsequently into the CO π^* orbital, from the sp^3 carbon in **8** relative to the sp^2 carbon in **9**.

Reactivity studies with cyclometalated complexes 1a and 5-L. As previously reported, **1a** activates simple silanes^{12,13} and stannanes¹⁴ *via* element–H bond activation. Thus, we sought to explore and compare the reactivities of **1a** and **5-L** toward small molecules, especially given the potential for these complexes to cleave a range of element–H bonds with subsequent reductive elimination of a C–H bond, to generate formally 16 electron $Cp^*(IXy)Ru$ and $Cp^*(IPr)Ru$ derivatives (Scheme 4).¹²

Scheme 4. Element–H bond activations by complex **1a**



Both **1a** and **5-L** were exposed to one atmosphere of H_2 at 24 °C in benzene. The reaction of **1a** with H_2 cleanly afforded $Cp^*(IXy)RuH_3$ (**10**; eq 5) in 75% yield.

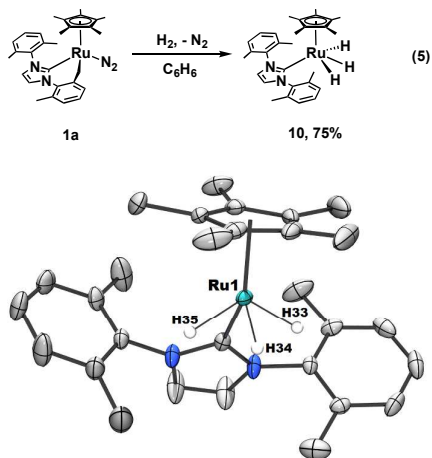
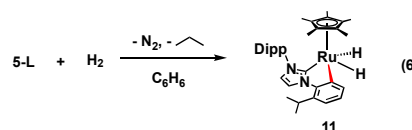


Figure 5. Molecular structure of **10** displaying thermal ellipsoids at the 50% probability level. Selected H atoms have been omitted for clarity.

This reaction likely proceeds by displacement of N_2 by H_2 , and oxidative addition to form the dihydride $Cp^*(IXy-H)RuH_2$. Then, reductive elimination of a C–H bond yields a 16-electron $Cp^*(IXy)RuH$ complex, to which a second equivalent of H_2 can bind to give the product. The structure of **10** was confirmed by single-crystal X-ray diffraction (Figure 5), which revealed a four-legged

piano stool geometry about the Ru center with a Ru–C(NHC) bond length of 2.027(3) Å and three Ru–H bond distances of 1.52(3), 1.52(3) and 1.66(4) Å. The hydride ligands were located in the difference electron density map and interligand distances between hydrides of 1.60(5), 1.64(5), and 2.74(5) Å suggest classical hydride bonding in the solid-state structure. The 1H NMR spectrum of **10** in toluene- d_8 at 24 °C exhibits a single hydride resonance at $\delta = -9.52$ ($T_1 = 424.6$ ms; –50 °C in toluene- d_8 ; 500.13 MHz).^{26, 27} The appearance of a single hydride resonance and its moderately slow relaxation time suggest that the three hydride ligands in **10** are classically-bound in the ground state and exchange rapidly, similar to those of $Cp^*(IMes)RuH_3$ and $Cp^*(IPr)RuH_3$ ($Cp^* = C_5Me_4Et$), as reported by Jones *et al.*²⁸

In contrast, the reaction of **5-L** with H_2 yielded the dihydride $Cp^*(IPr')RuH_2$ (**11**, eq. 6), which was characterized by NMR spectroscopy and elemental analysis. The 1H NMR spectrum of **11** exhibits a single resonance at –9.14 ppm (2 H) with T_1 of 104 ms (–30 °C in toluene- d_6 ; 500.13 MHz). The relatively small T_1 suggests that **11** should be classified as an elongated dihydrogen complex,²⁶ which possesses a significant interaction between two hydride ligands.



Thus, in contrast to the related reaction of **1a**, this transformation does not result in opening of the chelate ring. This discrepancy between **1a** and **5-L** likely results from the effect of chelate ring size (5- vs. 6-membered ring), and the Ru–C(sp^3) bond in **1a** being weaker than the Ru–C(sp^2) bond in **5-L**. The weaker Ru–C bond in **1a** is thus able to undergo C–H reductive elimination, and subsequently open a site for another oxidative addition, while the stronger Ru–C bond in **11** persists. In addition, unlike reactions of **5-L** with CO and $MesSiH_3$, no free propene was observed by 1H NMR upon treatment of **5-L** with dihydrogen, and instead, propane formation was observed, implicating **11** in the hydrogenation of propene.

The chelate rings in cyclometalated **1a** and **5-L** may in principle be opened by reactions with electrophiles. To investigate this possibility, the Lewis acid $B(C_6F_5)_3$, which is known to abstract alkylide and hydride ligands from metal complexes,²⁹ was employed. The reaction of **1a** with one equiv of $B(C_6F_5)_3$ in benzene at 24 °C cleanly yielded the zwitterionic compound $Cp^*Ru(IXy^-)$ (**12**; $IXy^- = 1-[2-((C_6F_5)_3BCH_2)C_6H_3-6-methyl]-3-(2,6-dimethylphenyl)imidazol-2-ylidene-1-yl]$) in 95% yield as a reddish-purple solid (eq 7). The ^{11}B NMR spectrum of **12** exhibits a sharp peak at –12.47 ppm, indicating the formation of a four-coordinate boron center derived from $B(C_6F_5)_3$. X-ray crystallography revealed that in **12** the $B(C_6F_5)_3$ moiety binds to the formerly metal-bound carbon atom in the $Cp^*(IXy-H)Ru$ fragment (Figure 6), with a C–B bond length of 1.663(13) Å. This structure features donation from

the *ipso* carbon of the benzylic entity (derived from a xylyl group of IXy) to the ruthenium center with a Ru–C(3) bond length of 2.420(9) Å. Moreover, on one of the two copies of **12** in the asymmetric unit, the methylene hydrogen atoms were found in the difference electron density map and refined independently. The close contact between the Ru atom and the center of the C4–H4a bond (2.31 Å), along with observation of upfield-shifted, diastereotopic protons at 0.84 and 0.44 ppm in the ^1H NMR spectrum, are indicative of a C–H agostic interaction that formally makes **12** an 18-electron complex.

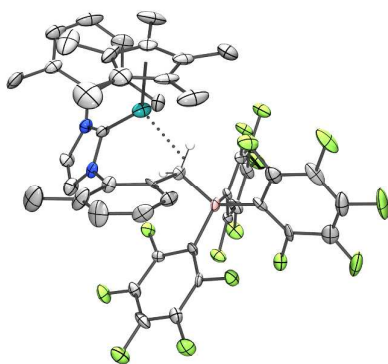
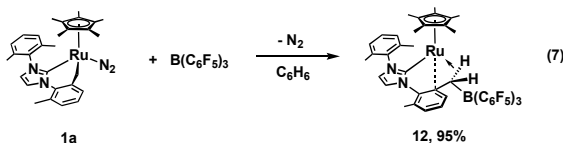


Figure 6. Molecular structure of one copy of **12** displaying thermal ellipsoids at the 50% probability level. Selected H atoms have been omitted for clarity.

Compared to the benzylic carbon in **1a**, decoordination of the cyclometalated aryl carbon in **5-L** to form a C–B bond seems less likely as the Ru–C(sp^2) bond is apparently stronger, and the IPr' ligand is more sterically demanding than IMes'. The observed reactivity confirms this prediction. Addition of $\text{B}(\text{C}_6\text{F}_5)_3$ to a benzene solution of **5-L** resulted in an immediate color change from pale yellow to blue. The ^1H NMR spectrum of the new product **13** in bromobenzene- d_5 exhibits a broad resonance at 4.10 ppm, attributed to the $\text{HB}(\text{C}_6\text{F}_5)_3^-$ anion, while three sets of doublets at 4.95, 4.09, 3.06 ppm provide evidence for coordination of an alkenyl group to ruthenium. High-resolution positive-ion-mode electrospray ionization mass spectrometry revealed the presence of $[\text{Cp}^*\text{Ru}(\text{IPr}')(\text{propene})] - \text{H}$ ($m/z = 623.2938$), further supporting formation of a cation that would result from hydride abstraction. The structure of **13**, confirmed by X-ray crystallography (Figure 7), reveals a formally 16-electron $[\text{Cp}^*\text{Ru}(\text{IPr}'')][\text{H}(\text{B}(\text{C}_6\text{F}_5)_3)]$ (IPr'' = 1-[2-($\text{CH}_2=\text{CHCH}_2$) C_6H_3 -6-isopropyl]-3-(2,6-diisopropyl)imidazol-2-ylidene-1-yl) complex (**13**; eq 8), in which the IPr'' ligand binds to ruthenium through both the central carbene carbon and an allyl substituent resulting from C–C bond formation. The bonding of the allyl fragment to ruthenium results in a Ru–C(1) bond length of 2.106(3) Å, a Ru–C_{olefin}(centroid) bond distance of 2.113 Å, and a C(5)–C(6) bond of 1.355(4) Å (Figure 7). A related ruthenium

complex $[\text{Cp}(\text{PPh}_3)\text{Ru}(1\text{-allyl-3-methylimidazol-2-ylidene})]\text{Cl}$ reported by Gandolfi *et al.*³⁰ exhibits a comparable Ru–C_{olefin}(centroid) bond distance of 2.101(5) Å and a slightly longer C–C(olefin) bond length of 1.374(11) Å, reflecting a higher degree of back donation from an electronic saturated 18 electron Ru complex.

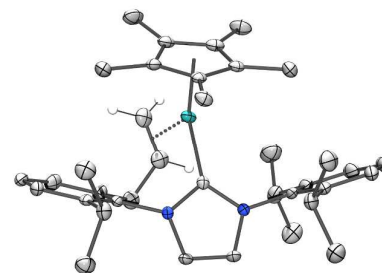
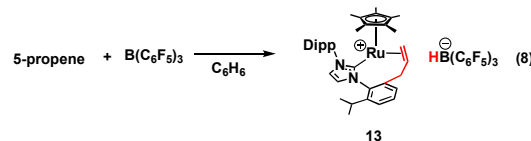


Figure 7. Crystal structure of **13** $[\text{Cp}^*\text{Ru}(\text{IPr}'')][\text{H}(\text{B}(\text{C}_6\text{F}_5)_3)] \cdot \text{C}_6\text{H}_5\text{F}$ displaying thermal ellipsoids at the 50% probability level. Selected H atoms, $\text{HB}(\text{C}_6\text{F}_5)_3^-$ counterion and solvent molecule have been omitted for clarity.

The allyl substituent of **13** is bonded to the formerly cyclometalated aryl carbon and likely results from insertion of a propene ligand into the Ru–C(aryl) bond in $\text{Cp}^*\text{Ru}(\text{IPr}')(\text{propene})$ (**5-propene**) upon hydride abstraction. The formation of **13** likely proceeds *via* hydride abstraction from the allylic carbon of the propene ligand in **5-propene** to yield an allyl ligand on a cationic Ru complex. Then, the allyl ligand undergoes migratory insertion into the Ru–C(aryl) bond to yield the product. No products associated with a reaction involving **5-N₂** were observed or isolated. This sequence represents an unusual pathway for C–C bond formation. Further studies of **13** are planned, since hybrid, chelating carbene ligands with tethered alkenyl groups can exhibit hemilability of the olefin substituent, and this property can be useful in catalytic applications including transfer hydrogenation³¹ and hydrosilation³².

Conclusion

In summary, we have demonstrated an unusual C–C bond activation, induced by an initial C–H bond activation to form a mixture of cyclometalated complexes, **5-L**, containing $\text{Cp}^*(\text{IPr}')\text{Ru}$ with a NHC-C(sp^2) ligand. Spectroscopy and reactivity studies reveal **5-L** to be composed of diastereomers of **5-propene** and a dinitrogen complex (**5-N₂**). In comparison, a similar ruthenium fragment containing a NHC-C(sp^3) chelating ligand, $\text{Cp}^*(\text{IXy-H})\text{Ru}$, is found to be more electron rich and capable of C–H reductive elimination in the presence of hydride ligands. The $\text{Cp}^*(\text{IPr}')\text{Ru}$ fragment undergoes an unusual C–C bond-forming reaction upon reaction

with $B(C_6F_5)_3$. The results described above highlight the substantial variations in chemical properties that can result from simple changes of electronic and steric properties in supporting ligands on ruthenium complexes. Further explorations of these complexes' ability to catalytically transform small molecules are ongoing.

Experimental section

General Procedures. All experiments were conducted under nitrogen using standard Schlenk techniques or in a N_2 -filled drybox. Nondeuterated solvents were distilled under N_2 from appropriate drying agents and stored in PTFE-valved flasks. Benzene- d_6 was dried by vacuum distillation from Na/K alloy. The compounds $Cp^*(IXy)RuCl$, $Cp^*(IXy-H)Ru(N_2)$ (complex **1a**),¹² and $Cp^*(IPr)RuCl$ ³³ were prepared according to literature procedures. All other chemicals were purchased from commercial sources and used without further purification. NMR spectra were recorded using Bruker AV-500 or AV-600 spectrometers equipped with a 5 mm BB probe. Spectra were recorded at room temperature and referenced to the residual protonated solvent for 1H NMR spectra. $^{13}C\{^1H\}$ NMR spectra were calibrated internally with the resonance for the solvent relative to tetramethylsilane. For $^{13}C\{^1H\}$ NMR spectra, resonances obscured by the solvent signal are omitted. ^{29}Si NMR spectra were referenced relative to a tetramethylsilane standard and obtained *via* 2D 1H ^{29}Si HMBC experiments unless specified otherwise. All spectra were recorded at room temperature unless otherwise noted. Complex multiplets are noted as "m" and broad resonances as "br". In $^{13}C\{^1H\}$ NMR spectra, resonances obscured by the solvent signal are omitted. Infrared spectra were recorded with analytically pure solid samples on a Bruker Alpha-P ATR using OPUS software (v. 6.5).

Observation of intermediate **4a**. Equimolar of $Cp^*(IPr)RuCl$ and $LiCH_2SiMe_3$ were mixed in 0.6 mL C_6D_6 , resulting a navy blue solution instantly, and the 1H NMR spectrum was taken within 5 minutes. 1H NMR (C_6D_6 , 600 MHz): δ 7.55 (d, $J_{HH} = 8.0$ Hz, 1 H), 7.33 – 7.20 (m, 3 H), 7.09 (d, $J_{HH} = 7.3$ Hz, 1 H), 6.99 (t, $J_{HH} = 7.3$ Hz, 1 H), 6.37 (br, 1 H, *NCHCHN*), 6.23 (br, 1 H, *NCHCHN*), 3.55 (septet, $J_{HH} = 6.8$ Hz, 1 H, *CHMe_2*), 2.99 (septet, $J_{HH} = 6.7$ Hz, 1 H, *CHMe_2*), 2.53 (septet, $J_{HH} = 6.7$ Hz, 1 H, *CHMe_2*), 2.02 (s, 3 H, *CHMe_2*), 1.73 (d, $J_{HH} = 7.2$ Hz, 3 H, *CHMe_2*), 1.50 (s, 15 H, C_5Me_5), 1.31 (d, $J_{HH} = 6.9$ Hz, 3 H, *CHMe_2*), 1.24 (d, $J_{HH} = 6.7$ Hz, 3 H, *CHMe_2*), 1.09 (d, $J_{HH} = 6.8$ Hz, 3 H, *CHMe_2*), 1.05 (d, $J_{HH} = 6.7$ Hz, 3 H, *CHMe_2*), 0.99 (d, $J_{HH} = 6.8$ Hz, 3 H, *CHMe_2*).

$Cp^*(IPr)Ru(L)$ (L = propene and N_2 , **5-L**). A 6 mL benzene solution of $Cp^*(IPr)RuCl$ (0.075 g, 0.11 mmol) and $LiCH_2SiMe_3$ (0.012 g, 0.13 mmol) was stirred at 24°C for 1 d. After removal of all volatile materials under vacuum, the resulting solid was extracted with 10 mL of pentane. The filtrate was dried under vacuum to afford **5-L** as a pale-yellow solid. Yield: 0.066 g. EI-MS: 624 (corresponding to $C_{37}H_{50}N_2Ru$). $\nu(N_2)$: 2093 cm^{-1} .

$Cp^*(IPr)(H)RuSiH_2Mes$ (**6**). A 3 mL benzene solution of $MesSiH_3$ (0.014 g, 0.09 mmol) was added to a 6 mL benzene solution of **5-L** (0.057 g), and the resulting reaction mixture was stirred at ambient temperature for 1 d. All volatile materials were removed under vacuum, and the resulting solid was extracted with 10 mL of pentane. Cooling the pentane solution down to -30 °C afforded colorless crystals. Yield: 0.043 g. 1H NMR (C_6D_6 , 600 MHz): δ 7.66 (d, $J_{HH} = 6.7$ Hz, 1 H), 7.61 (s, 1 H), 7.22 (br, 2 H), 7.12 (t, $J_{HH} = 7.1$ Hz, 1 H), 7.08 (br, 1 H), 6.99 (d, $J_{HH} = 6.7$ Hz, 1 H), 6.71 (br, 2 H), 6.63 (br, 1 H), 4.78 (s, $^1J_{SiH} = 172.5$ Hz, 1 H, *SiH*), 4.57 (s, $^1J_{SiH} = 183.2$ Hz, 1 H,

SiH), 3.45-3.39 (m, 2 H, *CHMe_2*), 2.40 (br, 1 H, *CHMe_2*), 2.19 (s, 3 H), 2.12 (s, 6 H), 1.50 (s, 15 H, C_5Me_5), 1.29-1.08 (m, 18 H, *CHMe_2*), -9.50 (s, 1 H, *RuH*). $^{13}C\{^1H\}$ NMR (C_6D_6 , 150.9 MHz): δ 197.1 (NCN), 169.0, 148.4, 147.5, 144.3, 143.9, 142.6, 138.8, 137.7, 136.1, 132.4, 130.5, 125.6, 125.4, 124.5, 124.4, 119.6, 117.9, 96.5 (C_5Me_5), 29.6, 29.1, 28.8, 28.6, 26.5, 25.4, 24.7, 23.6, 22.9, 22.2, 21.6, 10.6 (C_5Me_5). ^{29}Si NMR (C_6D_6 , 99.4 MHz): δ -32.7. Anal. Calcd for $C_{43}H_{58}N_2SiRu$: C, 70.55; H, 7.99; N, 3.83. Found: C, 70.88; H, 7.99; N, 4.06.

$[Cp^*Ru(IXy-2H)][K(18-crown-6)]$ (**7**). A 3 mL toluene solution of KCH_2Ph (0.034 g, 0.26 mmol) and 18-crown-6 (0.069 g, 0.26 mmol) was slowly added to a 10 mL toluene solution of **1a** (0.134 g, 0.25 mmol). The brown precipitate was observed immediately upon addition. The resulting solution was stirred at 24 °C for 1 h. The resulting brown solid was collected by decanting the solution, washing three times with 10 mL of pentane, and drying under vacuum to afford analytically pure product. Yield: 0.213 g (97%). 1H NMR (THF- d_8 , 600 MHz): δ 7.14 (s, 2 H, *NCHCHN*), 6.65 (d, $J_{HH} = 7.24$ Hz, 2 H), 6.54 (t, $J_{HH} = 7.2$ Hz, 2 H), 6.26 (d, $J_{HH} = 7.2$ Hz, 2 H), 3.53 (s, 24 H, H's of 18-C-6), 2.31 (s, 2 H, *RuCH_2*), 2.17 (s, 6 H, *xylyl's Me*), 1.93 (br, 2 H, *RuCH_2*), 1.59 (s, 15 H, C_5Me_5). $^{13}C\{^1H\}$ NMR (C_6D_6 , 150.9 MHz): δ 178.2 (NCN), 139.9, 129.7, 126.9, 124.1, 121.7, 120.3, 117.2, 81.6 (C_5Me_5), 71.2 (18-C-6), 21.6, 19.9, 11.0 (C_5Me_5). Anal. Calcd for $C_{41}H_{57}N_2O_6KRu$: C, 60.49; H, 7.06; N, 3.44. Found: C, 60.76; H, 7.07; N, 3.30.

$Cp^*(IXy-H)Ru(CO)$ (**8**). A 10 mL benzene solution of **1a** (0.049 g, 0.09 mmol) was subjected to three freeze-pump-thaw cycles, and then was exposed to 1 atm of CO and stirred for 1 h to give a yellow solution. All volatile materials were removed under vacuum, and the resulting solid was extracted with 10 mL of pentane. Concentrating the pentane solution to ca. 5 mL and cooling it down to -30 °C afforded a pale-yellow solid. Yield: 0.035 g (71%). $\nu(CO) = 1868$ cm^{-1} . 1H NMR (C_6D_6 , 600 MHz): δ 7.21 (d, $J_{HH} = 7.5$ Hz, 1 H), 7.15-7.10 (m, 2 H), 7.01 (d, $J_{HH} = 7.3$ Hz, 1 H), 6.93 (t, $J_{HH} = 7.5$ Hz, 1 H), 6.72 (d, $J_{HH} = 7.5$ Hz, 1 H), 6.69 (d, $J_{HH} = 1.9$ Hz, 1 H, *NCHCHN*), 6.03 (d, $J_{HH} = 1.9$ Hz, 1 H, *NCHCHN*), 2.77 (d, $J_{HH} = 10.9$ Hz, 1 H, *CH_2*), 2.12 (s, 3 H, *xylyl's Me*), 2.06 (s, 6 H, *xylyl's Me*), 1.88 (d, $J_{HH} = 10.9$ Hz, 1 H, *CH_2*), 1.51 (s, 15 H, C_5Me_5). $^{13}C\{^1H\}$ NMR (C_6D_6 , 150.9 MHz): δ 210.1 (CO), 196.4 (NCN), 151.0, 139.5, 139.1, 138.1, 134.6, 128.7, 127.0, 125.7, 125.3, 124.0, 121.3, 121.1, 93.8 (C_5Me_5), 19.0, 18.6, 18.5, 9.5 (C_5Me_5). Anal. Calcd for $C_{30}H_{34}N_2ORu$: C, 66.77; H, 6.35; N, 5.19. Found: C, 66.71; H, 6.14; N, 5.08.

$Cp^*(IPr)Ru(CO)$ (**9**). A 10 mL benzene solution of **5-L** (0.090 g) was subjected to three freeze-pump-thaw cycles, and then was exposed to 1 atm of CO and stirred for 4 h to give a yellow solution. All volatile materials were removed under vacuum, and the resulting solid was extracted with 10 mL of pentane. Concentrating the pentane solution to ca. 5 mL and cooling it down to -30 °C afforded a pale-yellow solid. Yield: 0.075 g. $\nu(CO) = 1908$ cm^{-1} . 1H NMR (C_6D_6 , 600 MHz): δ 7.97 (d, $J_{HH} = 7.3$ Hz, 1 H), 7.59 (d, $J_{HH} = 2.03$ Hz, 1 H, *NCHCHN*), 7.29-7.25 (m, 3 H), 7.13-7.08 (m, 3 H), 6.63 (d, $J_{HH} = 2.0$ Hz, 1 H, *NCHCHN*), 3.59 (septet, $J_{HH} = 6.9$ Hz, 1 H, *CHMe_2*), 3.36 (septet, $J_{HH} = 6.9$ Hz, 1 H, *CHMe_2*), 2.70 (septet, $J_{HH} = 6.9$ Hz, 1 H, *CHMe_2*), 1.60 (s, 15 H, C_5Me_5), 1.58 (d, $J_{HH} = 6.8$ Hz, 3 H, *CHMe_2*), 1.22 (d, $J_{HH} = 6.8$ Hz, 3 H, *CHMe_2*), 1.17-1.12 (m, 9 H, *CHMe_2*), 1.04 (d, $J_{HH} = 6.9$ Hz, 3 H, *CHMe_2*). $^{13}C\{^1H\}$ NMR (C_6D_6 , 150.9 MHz): δ 205.1 (CO), 193.9 (NCN), 165.0, 145.8, 146.6, 145.4, 139.8, 137.6, 133.0, 130.4, 125.1, 124.9, 124.8, 124.5, 120.2, 118.6, 95.8 (C_5Me_5), 29.4, 29.1, 28.8, 28.1, 26.6, 24.8, 23.7, 23.4, 23.1, 10.9 (C_5Me_5). Anal. Calcd for $C_{35}H_{44}N_2ORu$: C, 68.94; H, 7.27; N, 4.59. Found: C, 69.06; H, 7.51; N, 4.52.

Cp*(IXy)RuH₃ (**10**). A 10 mL benzene solution of **1a** (0.053 g, 0.10 mmol) was subjected to three freeze-pump-thaw cycles, and then was exposed to 1 atm of H₂ and stirred for 1 h to give a yellow solution. All volatile materials were removed under vacuum, and the resulting solid was extracted with 10 mL of pentane. Concentrating the pentane solution to ca. 5 mL and cooling to -30 °C afforded a pale-yellow solid. Yield: 0.038 g (75%). ¹H NMR (C₆D₆, 600 MHz): δ 7.12 (t, *J*_{HH} = 6.9 Hz, 2 H), 7.0 (d, *J*_{HH} = 6.9 Hz, 4 H), 6.05 (s, 2 H, NCHCHN), 2.11 (s, 12 H, xlyl's Me), 1.82 (s, 15 H, C₅Me₅), -9.42 (s, 3 H, RuH). ¹H NMR (toluene-*d*₈, 600 MHz): δ 7.09 (t, *J*_{HH} = 7.1 Hz, 2 H), 7.02 (d, *J*_{HH} = 7.6 Hz, 4 H), 6.06 (s, 2 H, NCHCHN), 2.08 (s, 12 H, xlyl's Me), 1.78 (s, 15 H, C₅Me₅), -9.53 (s, 2 H, RuH). ¹³C{¹H} NMR (C₆D₆, 150.9 MHz): δ 194.5 (NCN), 142.7, 137.0, 128.8, 128.7, 120.8, 93.7 (C₅Me₅), 19.5, 13.1 (C₅Me₅). Anal. Calcd for C₂₉H₃₈N₂Ru: C, 67.54; H, 7.43, N, 5.43. Found: C, 67.54, H, 7.35, N, 5.37.

Cp*(IPr')RuH₂ (**11**). A 5 mL benzene solution of **5-L** (0.042 g) was subjected to three freeze-pump-thaw cycles, and then was exposed to 1 atm of H₂ and stirred for 2 h to give a yellow solution. All volatile materials were removed under vacuum, and the resulting solid was extracted with 10 mL of pentane. Concentrating the pentane solution to ca. 3 mL and cooling to -30 °C afforded a pale-yellow solid. Yield: 0.024 g. ¹H NMR (C₆D₆, 600 MHz): δ 8.21 (d, *J*_{HH} = 7.5 Hz, 1 H), 7.53 (d, *J*_{HH} = 2.2 Hz, 1 H, NCHCHN), 7.32-7.26 (m, 3 H), 7.1-7.14 (m, 2 H), 6.62 (d, *J*_{HH} = 2.2 Hz, 1 H, NCHCHN), 3.43 (septet, *J*_{HH} = 6.4 Hz, 1 H, CHMe₂), 2.99-2.89 (m, 2 H, CHMe₂), 1.66 (s, 15 H, C₅Me₅), 1.51 (d, *J*_{HH} = 6.9 Hz, 3 H, CHMe₂), 1.33 (d, *J*_{HH} = 6.9 Hz, 3 H, CHMe₂), 1.22 (d, *J*_{HH} = 6.9 Hz, 6 H, CHMe₂), 1.18 (d, *J*_{HH} = 6.9 Hz, 3 H, CHMe₂), 0.91 (d, *J*_{HH} = 6.9 Hz, 3 H, CHMe₂), -9.14 (s, 2 H, RuH). ¹³C{¹H} NMR (C₆D₆, 150.9 MHz): δ 200.3 (NCN), 168.1, 149.0, 146.6, 144.4, 139.8, 138.3, 132.9, 130.2, 125.4, 124.1, 123.7, 123.2, 119.5, 117.7, 96.5 (C₅Me₅), 29.8, 29.1, 28.9, 27.9, 26.8, 25.1, 23.7, 23.2, 22.6, 11.6 (C₅Me₅). Anal. Calcd for C₃₄H₄₆N₂Ru: C, 69.95; H, 7.94, N, 4.80. Found: C, 69.62, H, 7.80, N, 4.75.

Cp*Ru(IXy"") (**12**, IXy" = 1-[2-((C₆F₅)₃BCH₂)C₆H₃-6-methyl]-3-(2,6-dimethylphenyl)imidazol-2-ylidene-1-yl). A 3 mL benzene solution of B(C₆F₅)₃ (0.036 g, 0.07 mmol) was added to a 6 mL benzene solution of **1a** (0.036 g, 0.07 mmol), and the resulting reaction mixture was stirred at ambient temperature for 3 h. All volatile materials were removed under vacuum, and the resulting solid was washed with 5 mL of pentane three times and then dried under vacuum to afford a purple powder. Yield: 0.090g (95%) ¹H NMR (C₆D₆, 600 MHz): δ 7.80 (d, *J*_{HH} = 7.9 Hz, 1 H), 6.97 (t, *J*_{HH} = 7.6 Hz, 1 H), 6.85 (d, *J*_{HH} = 7.9 Hz, 1 H), 6.81 (d, *J*_{HH} = 7.6 Hz, 1 H), 6.74 (t, *J*_{HH} = 7.9 Hz, 1 H), 6.64 (d, *J*_{HH} = 7.3 Hz, 1 H), 6.08 (d, *J*_{HH} = 1.9 Hz, 1 H, NCHCHN), 5.85 (d, *J*_{HH} = 1.9 Hz, 1 H, NCHCHN), 1.99 (s, 3 H, xlyl's Me), 1.73 (s, 3 H, xlyl's Me), 1.51 (s, 3 H, xlyl's Me), 0.89 (s, 15 H, C₅Me₅), 0.84 (br, 1 H, CH₂), 0.44 (br, 1 H, CH₂). ¹³C{¹H} NMR (C₆D₆, 150.9 MHz): δ 179.2 (NCN), 138.5, 137.1, 135.8, 134.2, 131.1, 129.5, 129.4, 129.2, 126.5, 125.7, 124.1, 120.1, 77.4 (C₅Me₅), 18.4, 17.5, 17.4, 10.0, 9.3 (C₅Me₅). ¹¹B{¹H} NMR (C₆D₆, 152.5 MHz): δ -12.47. ¹⁹F NMR (C₆D₆, 376.5 MHz): δ 129.1 (d, *J* = 24.4 Hz), 160.3 (t, *J* = 21.2 Hz), 164.4 (t, *J* = 21.2 Hz). Anal. Calcd for C₄₇H₃₄BF₁₅N₂ORu: C, 55.15; H, 3.35; N, 2.74. Found: C, 55.59; H, 3.57; N, 2.60.

[Cp*Ru(IPr'')][HB(C₆F₅)₃] (**13**). A 3 mL benzene solution of B(C₆F₅)₃ (0.036 g, 0.06 mmol) was added to a 6 mL benzene solution of **5-L** (0.037 g, 0.06 mmol). After stirring for 1h at room temperature, 15 mL of pentane was added to the navy blue solution, and the reaction vessel was placed in the -30 °C freezer. After 1 h, a blue oil settled to the bottom of the vial. The solution was carefully decanted, and the resulting blue oil was dried under vacuum for 1 h to afford **13** as a blue solid. Yield: 0.045 g. ¹H NMR (C₆D₅Br, 600

MHz): δ 7.53 (t, *J*_{HH} = 7.6 Hz, 1 H), 7.23-7.17 (m, 6 H), 6.86 (d, *J*_{HH} = 6.5 Hz, 1 H), 4.95 (d, *J*_{HH} = 10.5 Hz, 1 H), 4.44 (br, 1 H, HB(C₆F₅)₃), 4.09 (d, *J*_{HH} = 15.6 Hz, 1 H), 3.06 (d, *J*_{HH} = 13.9 Hz, 1 H), 2.97-2.92 (m, 3 H, CHMe₂), 2.20-2.15 (m, 2 H), 1.57 (d, *J*_{HH} = 6.7 Hz, 3 H, CHMe₂), 1.40 (d, *J*_{HH} = 6.5 Hz, 3 H, CHMe₂), 1.36 (d, *J*_{HH} = 6.5 Hz, 3 H, CHMe₂), 1.26 (d, *J*_{HH} = 6.7 Hz, 3 H, CHMe₂), 1.05 (d, *J*_{HH} = 6.7 Hz, 3 H, CHMe₂), 0.83 (s, 15 H, C₅Me₅), 0.76 (d, *J*_{HH} = 6.5 Hz, 3 H, CHMe₂). HR-ESI-MS(+) calcd for C₃₇H₄₉N₂Ru: 623.2939; found: 623.2938

Computational Details. Calculations using Gaussian 09 (G09) suite of programs were performed in the molecular graphics and computing facility of the College of Chemistry, University of California, Berkeley. The geometry optimizations were carried out using the B3LYP functional.³⁴⁻³⁷ Ru was represented with the effective core potential (ECP) from the Stuttgart group and the associated optimal basis sets.³⁸ All other atoms were represented by the 6-31G(d,p) basis set. The nature of the extrema as minima was confirmed with analytical frequency calculations. The connection between transition states, reactants and products was verified by IRC calculations. Statistical mechanics calculations of thermal and entropic effects were carried out using the rigid rotor/harmonic oscillator approximations at room temperature and 1 atm. The Gibbs energies, G, were calculated at 298.15 K and 1 atm. Coordinates of computed structures as a .xyz file is available in Supporting Information.

X-ray Crystallography Details. X-ray diffraction data were collected using Bruker AXS three-circle diffractometers coupled to a CCD detector with either QUAZAR multilayer mirror- or graphite-monochromated Mo K α radiation (λ = 0.71073 Å). The structures were solved using Superflip (V04/17/13) or SHELXT-2014, and using SHELXL-2014, refined against F² on all data by full-matrix least squares. All non-hydrogen atoms were refined anisotropically; hydrogen atoms were included at their geometrically calculated positions and refined using a riding model except hydrogen atoms connected to ruthenium or silicon, which were located from the electron difference map. CCDC 1842934 (**6**), CCDC 1842935 (**7**), CCDC 1842931 (**10**), CCDC 1842933 (**12**) and CCDC 1842932 (**13**) contain the supplementary crystallographic data for this paper. These data can be obtained free of charge from The Cambridge Crystallographic Data Centre via www.ccdc.cam.ac.uk/data_request/cif.

Conflicts of interest

There are no conflicts to declare.

Acknowledgements

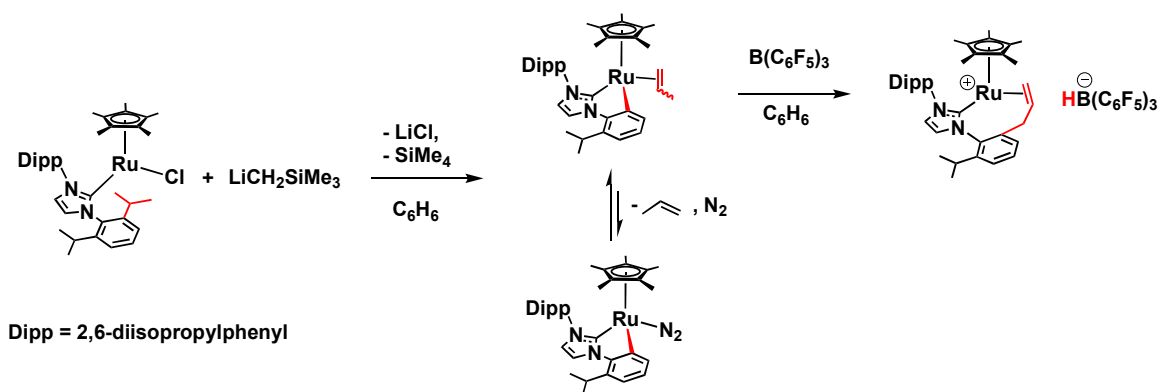
This work was funded by the National Science Foundation under grant no. CHE-1566538. The UC Berkeley Molecular Graphics and Computing Facility is supported by the National Institutes of Health under grant no. S10-OD023532; UC Berkeley ChexRay is funded by the National Institutes of Health under grant no. S10-RR027172.

Notes and references

1. M. I. Bruce, *Angew. Chem. Int. Ed. Engl.*, 1977, **16**, 73-86.
2. M. Albrecht, *Chem. Rev.*, 2010, **110**, 576-623.
3. I. Omae, *Coord. Chem. Rev.*, 2004, **248**, 995-1023.
4. I. Omae, *Coord. Chem. Rev.*, 2014, **280**, 84-95.

5. Z. Mo, Y. Liu and L. Deng, *Angew. Chem. Int. Ed.*, 2013, **52**, 10845-10849.
6. J.-P. Djukic, J.-B. Sortais, L. Barloy and M. Pfeffer, *Eur. J. Inorg. Chem.*, 2009, **2009**, 817-853.
7. P. G. Bomben, K. C. D. Robson, B. D. Koivisto and C. P. Berlinguette, *Coord. Chem. Rev.*, 2012, **256**, 1438-1450.
8. S. Burling, B. M. Paine, D. Nama, V. S. Brown, M. F. Mahon, T. J. Prior, P. S. Pregosin, M. K. Whittlesey and J. M. J. Williams, *J. Am. Chem. Soc.*, 2007, **129**, 1987-1995.
9. K. Endo, M. B. Herbert and R. H. Grubbs, *Organometallics*, 2013, **32**, 5128-5135.
10. Z. Ouyang and L. Deng, *Organometallics*, 2013, **32**, 7268-7271.
11. J. Sun, L. Luo, Y. Luo and L. Deng, *Angew. Chem. Int. Ed.*, 2017, **56**, 2720-2724.
12. H.-J. Liu, C. Raynaud, O. Eisenstein and T. D. Tilley, *J. Am. Chem. Soc.*, 2014, **136**, 11473-11482.
13. H.-J. Liu, C. Landis, C. Raynaud, O. Eisenstein and T. D. Tilley, *J. Am. Chem. Soc.*, 2015, **137**, 9186-9194.
14. H.-J. Liu, J. Guihaumé, T. Davin, C. Raynaud, O. Eisenstein and T. D. Tilley, *J. Am. Chem. Soc.*, 2014, **136**, 13991-13994.
15. R. F. R. Jazzar, S. A. Macgregor, M. F. Mahon, S. P. Richards and M. K. Whittlesey, *J. Am. Chem. Soc.*, 2002, **124**, 4944-4945.
16. M. J. Chilvers, R. F. R. Jazzar, M. F. Mahon and M. K. Whittlesey, *Adv. Synth. Catal.*, 2003, **345**, 1111-1114.
17. S. Burling, M. F. Mahon, B. M. Paine, M. K. Whittlesey and J. M. J. Williams, *Organometallics*, 2004, **23**, 4537-4539.
18. T. Bolaño, M. L. Buil, M. A. Esteruelas, S. Izquierdo, R. Lalrempuia, M. Oliván and E. Oñate, *Organometallics*, 2010, **29**, 4517-4523.
19. R. Waterman, P. G. Hayes and T. D. Tilley, *Acc. Chem. Res.*, 2007, **40**, 712-719.
20. G. R. Fulmer, A. J. M. Miller, N. H. Sherden, H. E. Gottlieb, A. Nudelman, B. M. Stoltz, J. E. Bercaw and K. I. Goldberg, *Organometallics*, 2010, **29**, 2176-2179.
21. V. K. Dioumaev, L. J. Procopio, P. J. Carroll and D. H. Berry, *J. Am. Chem. Soc.*, 2003, **125**, 8043-8058.
22. F. R. Lemke, *J. Am. Chem. Soc.*, 1994, **116**, 11183-11184.
23. M. E. Fasulo, P. B. Glaser and T. D. Tilley, *Organometallics*, 2011, **30**, 5524-5531.
24. H.-J. Liu, M. S. Ziegler and T. D. Tilley, *Polyhedron*, 2014, **84**, 203-208.
25. S. Kronig, E. Theuergarten, C. G. Daniliuc, P. G. Jones and M. Tamm, *Angew. Chem. Int. Ed.*, 2012, **51**, 3240-3244.
26. P. G. Jessop and R. H. Morris, *Coord. Chem. Rev.*, 1992, **121**, 155-284.
27. R. H. Morris, *Coord. Chem. Rev.*, 2008, **252**, 2381-2394.
28. A. L. Jones, G. S. McGrady, P. Sirsch and J. W. Steed, *Chem. Commun.*, 2005, DOI: 10.1039/B512760B, 5994-5996.
29. P. G. Hayes, Z. Xu, C. Beddie, J. M. Keith, M. B. Hall and T. D. Tilley, *J. Am. Chem. Soc.*, 2013, **135**, 11780-11783.
30. C. Gandolfi, M. Heckenroth, A. Neels, G. Laurency and M. Albrecht, *Organometallics*, 2009, **28**, 5112-5121.
31. R. Corberán, M. Sanaú and E. Peris, *Organometallics*, 2007, **26**, 3492-3498.
32. N. Ding, W. Zhang and T. S. A. Hor, *Dalton Trans.*, 2012, **41**, 5988-5994.
33. L. Jafarpour, E. D. Stevens and S. P. Nolan, *J. Organomet. Chem.*, 2000, **606**, 49-54.
34. A. D. Becke, *J. Chem. Phys.*, 1993, **98**, 5648-5652.
35. C. Lee, W. Yang and R. G. Parr, *Phys. Rev. B*, 1988, **37**, 785-789.
36. P. J. Stephens, F. J. Devlin, C. F. Chabalowski and M. J. Frisch, *J. Phys. Chem.*, 1994, **98**, 11623-11627.
37. S. H. Vosko, L. Wilk and M. Nusair, *Can. J. Phys.*, 1980, **58**, 1200-1211.
38. D. Andrae, U. Häußermann, M. Dolg, H. Stoll and H. Preuß, *Theor. Chim. Acta*, 1990, **77**, 123-141.

1



Dehydrochlorination of Cp^{*}Ru(IPr)Cl leads to an unusual C–C bond activation, yielding a cyclometalated Ru complex bearing an NHC–C(sp²) ligand. Reactivity studies of cyclometalated Ru complexes were explored.